Supplementary information

Novel layered solid oxide fuel cell with multiple-twinned $Ni_{0.8}Co_{0.2}$ nanoparticles: the key to thermally independent CO_2 utilization and power-chemical cogeneration

Bin Hua [a], Ning Yan [b], Meng Li [c], Ya-qian Zhang [a], Yi-fei Sun [a], Jian Li [c], Thomas Etsell [a], Partha Sarkar [a, d], Karl Chuang [a], Jing-li Luo [a]

[a] Department of Chemical and Materials Engineering, University of Alberta, Edmonton, Alberta, T6G 2V4, Canada, Tel.: +1 780 492 2232; fax: +1 780 492 2881. E-mail address: jingli.luo@ualberta.ca (J.-L. Luo)

[b] Van't Hoff Institute for Molecular Sciences (HIMS), University of Amsterdam, Amsterdam, 1098XH, The Netherlands, Tel.: +31 20 492 6468. E-mail address: n.yan@uva.nl

[c] Center for Fuel Cell Innovation, School of Materials Science and Engineering, State Key Laboratory of Material Processing and Die & Mould Technology, Huazhong University of Science and Technology, Wuhan, Hubei, 430074, China

[d] Environment & Carbon Management Division, Alberta Innovates-Technology Futures, Edmonton, Alberta, T6N 1E4, Canada

Methods

Preparation of BZCYYb powder

BZCYYb powder with two distinct particle sizes was prepared using two different methods. For the solid-state reaction (SSR) process, stoichiometric amounts of $BaCO_3$, ZrO_2, CeO_2, Y_2O_3 and Yb_2O_3 powders were initially mixed and ball-milled in isopropyl alcohol, followed by calcination at 1100 °C for 10 h. The wet ball-milling and calcination steps were repeated until a pure perovskite phase was obtained. For the aqueous sol-gel process, stoichiometric amounts of $Ba(NO_3)_2$, zirconyl nitrate hydrate, $Ce(NO_3)_3{\cdot}6H_2O$, $Y(NO_3)_3{\cdot}6H_2O$ and $Yb(NO_3)_3{\cdot}5H_2O$ were initially dissolved in distilled water in a beaker, suitable amounts of EDTA and citric acid were added into the solution sequentially as chelating agents. The aqueous solution was heated to 80 °C with vigorous agitation until a viscous gel was formed. Then the beaker was transferred to an oven and was dried at 300 °C to form a black foamy intermediate product. This foam was ground into fine powder and then calcined at 1100 °C for 5 h in air to obtain BZCYYb powder. In order to evaluate the stability of BZCYYb in different feedstocks at high temperature, the BZCYYb powder was placed in a crucible that was then situated in a quartz tube subjected to either CH_4-CO_2 or H_2-CO treatment.

Preparation of NBCaC cathode

To prepare $NdBa_{0.75}Ca_{0.25}Co_2O_{5+\delta}$ (NBCaC) cathode, stoichiometric amounts of $Nd(NO_3)_3{\cdot}6H_2O$, $Ca(NO_3)_2{\cdot}4H_2O$, $Ba(NO_3)_2$ and $Co(NO_3)_3{\cdot}6H_2O$ were dissolved in

distilled water with ethylene glycol/citric acid added as the chelating agent. After the similar drying and grinding processes as that for BZCYYb preparation, the obtained powder was finally calcined in air at 900 °C for 5 h to form a layered perovskite NBCaC.

Preparation of the NiCo-LDC catalyst

NiCo-LDC catalyst was prepared by a glycine-nitrate auto combustion process (GNP). Initially, $Ni(NO_3)_2 \cdot 6H_2O$, $Co(NO_3)_2 \cdot 6H_2O$, $La(NO_3)_4 \cdot 6H_2O$ and $Ce(NO_3)_3 \cdot 6H_2O$ were dissolved in distilled water at a molar ratio of 6:1:2:8. Then glycine was added as both the chelating agent and the fuel. This solution was then heated on a hot-plate at 200 °C till auto-combustion occurred. The collected powder was finally calcined at 800 °C for 2 h to remove residual carbon and to form $Ni_{0.8}Co_{0.2}O$-$La_{0.2}Ce_{0.8}O_{1.9}$ (NiCoO-LDC) powder. NiCo-LDC catalyst was obtained via an *in situ* reduced in H_2 during the designated experiment.

In addition to the GNP method, we also prepared NiCo-LDC catalyst through a conventional wet-impregnation method. Firstly, $La_{0.2}Ce_{0.8}O_{1.9}$ (LDC) nano powder was prepared via the GNP method detailed above. Stoichiometric amounts of $Ni(NO_3)_2 \cdot 6H_2O$ and $Co(NO_3)_2 \cdot 6H_2O$ were dissolved in distilled water in a beaker. Sequentially, suitable amount of LDC nano powder was added into the solution under gentle agitation. The weight ratio of NiCo: LDC was also kept at 19.5:80.5. The suspension was then stirred and dried in a water bath at 80 ^oC. After water evaporation, the obtained powder was calcined at 800 °C for 2 h.

Cell fabrication

The anode-supported cells were prepared by using a dry pressing-spin coating-sintering process. To prepare the anode support, the powder mixture, containing NiO and SSR-derived BZCYYb at a weight ratio of 65:35, was ball-milled in isopropyl alcohol with 10 wt% corn starch as the pore former. After homogenization and drying, 1 g of the mixed powder was used to fabricate the anode support substrate using the dry pressing in a cylindrical die. A sequential 2 h pre-sintering at 1050 °C was applied to acquire strong substrates.

The thin BZCYYb electrolyte film on the NiO-BZCYYb anode substrate was prepared by an optimized slurry coating technique. Initially, GNP-derived BZCYYb-containing slurry was prepared by dispersing 2 g BZCYYb powder in 6 g ethanol in a vial. 0.04 g cellulose and 1g triethanolamine were added as the binder and the dispersant, respectively. A homogenous slurry was then obtained using an ultrasonic processor in which the vial was cooled using a water bath. BZCYYb membrane then was prepared by spin coating the BZCYYb suspension. The thickness of the BZCYYb membrane was controlled by the time of coating. Finally, the electrolyte coated substrate was densified at 1420 °C for 5 h.

To prepare the cathode layer, NBCaC-BZCYYb (GNP derived, weight ratio is 60:40) paste was prepared by adding suitable amount of home-made binder and then ground using a mortar-pestle. The paste was brush-painted on the surface of the sintered BZCYYb electrolyte with an area of 0.316 cm^2. The obtained membrane electrolyte assembly was finally calcined in air at 950 °C for 4 h to complete the

fabrication of the anode-supported cell. For the layered H-SOFC, The NiCoO-LDC layered was also prepared using the paste method via brushing the NiCoO-LDC paste on the anode support surface of the cell, followed by a calcination at 900 ºC in air for 2 h.

Preparation of the NBCaC-BZCYYb and NiCo-LDC catalyst slurries

The cathode and the NiCoO-LDC pastes were prepared by ball milling the powder and a home-made binder with a weight ratio of 50:50 for 1 h. The home-made binder was prepared via mixing 4 wt. % cellulose and 96 wt. % terpineol. The full dissolution of cellulose was acquired by heating the mixture to 80 °C under vigorous agitation.

CO_2-TPD

The CO_2-TPD (temperature-programmed desorption) was carried out to test the effect of the preparation method on the surface basicity of the NiCo-LDC catalysts. The samples were first treated in Ar at 500 °C for 1h to remove the absorbed species, and then cooled to room temperature, followed by exposing to CO_2 for 2h. The treated samples were purged with Ar at room temperature for 1h and heated linearly at 10-800 °C in a constant flow of Ar. The CO_2 signal was monitored and recorded continuously as a function of the temperature by the QIC-20 (Atmospheric Gas Analysis System).

Table S1. The specifications of chemicals.

Chemical formulas or Names	Supplier	Purity
$BaCO_3$	Fisher Scientific Company	99.0 % +
ZrO_2	Sigma-aldrich	99.99%
CeO_2	ACROS ORGANICS	99.9%
Y_2O_3	Fisher Scientific Acros	99.99%
Yb_2O_3	ACROS ORGANICS	99.99%
$Ba(NO_3)_2$	ACROS ORGANICS	99 % +
Zirconyl nitrate hydrate	ACROS ORGANICS	99.5 %
$Ce(NO_3)_3 \cdot 6H_2O$	ACROS ORGANICS	99.5 %
$Y(NO_3)_3 \cdot 6H_2O$	ACROS ORGANICS	99.9 %
$Yb(NO_3)_3 \cdot 5H_2O$	Fisher Scientific Acros	99.9%
$C_{10}H_{16}N_2O_8$ (EDTA)	Fisher Scientific Acros	99.5%
$C_6H_8O_7$ (Citric acid)	Fisher Scientific Company	99.5%
$Nd(NO_3)_3 \cdot 6H_2O$	Sigma-aldrich	99.9%
$Ca(NO_3)_2 \cdot 4H_2O$	ACROS ORGANICS	99%
$Co(NO_3)_3 \cdot 6H_2O$	ACROS ORGANICS	99% +
$Ni(NO_3)_2 \cdot 6H_2O$	Fisher Scientific Company	99.9%
$La(NO_3)_4 \cdot 6H_2O$	ACROS ORGANICS	99.995%
NiO	Fisher Scientific Company	97%
C_3H_8O (Isopropyl alcohol)	Fisher Scientific Company	68.0 to 72.0%
C_2H_6O (Ethanol)	Fisher Scientific Company	90%
$C_2H_6O_2$ (Ethylene glycol)	Fisher Scientific Company	99% +
Cellulose	ACROS ORGANICS	99%
Triethanolamine	ACROS ORGANICS	99% +
terpineol	ACROS ORGANICS	99% +

Results and discussions

Figure S1

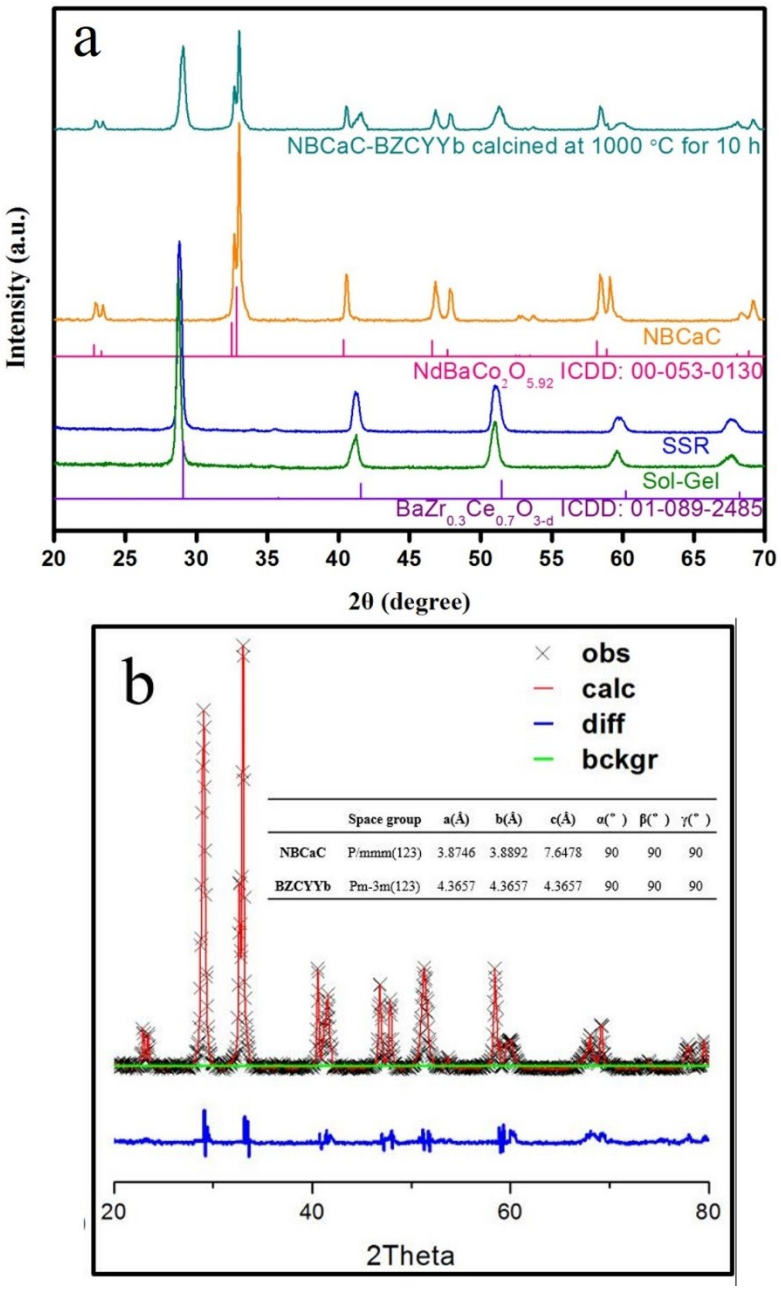

Figure S1. (a) XRD patterns of as-synthesized BZCYYb, NBCaC and their mixture co-fired at 1000 °C for 10 h; (b) the Rietveld analysis of BZCYYb-NBCaC mixture calcined at 1000 °C

X-ray diffraction patterns in Fig. S1 indicate that as-synthesized BZCYYb and NBCaC powders were single-phase perovskite. They also show excellent

compatibility since no extra peaks or splitting of main reflections were observed in the BZCYYb-NBCaC mixture calcined at 1000 °C, indicating that no apparent chemical reaction had occurred during either cathode preparation or under fuel cell operating condition. According to the Rietveld analysis, the weight ratio of BZCYYb/NBCaC is 37.4/62.6 after calcination, which is similar to the as-mixed powder (BZCYYb/NBCaC is 40.0/60.0).

Figure S2

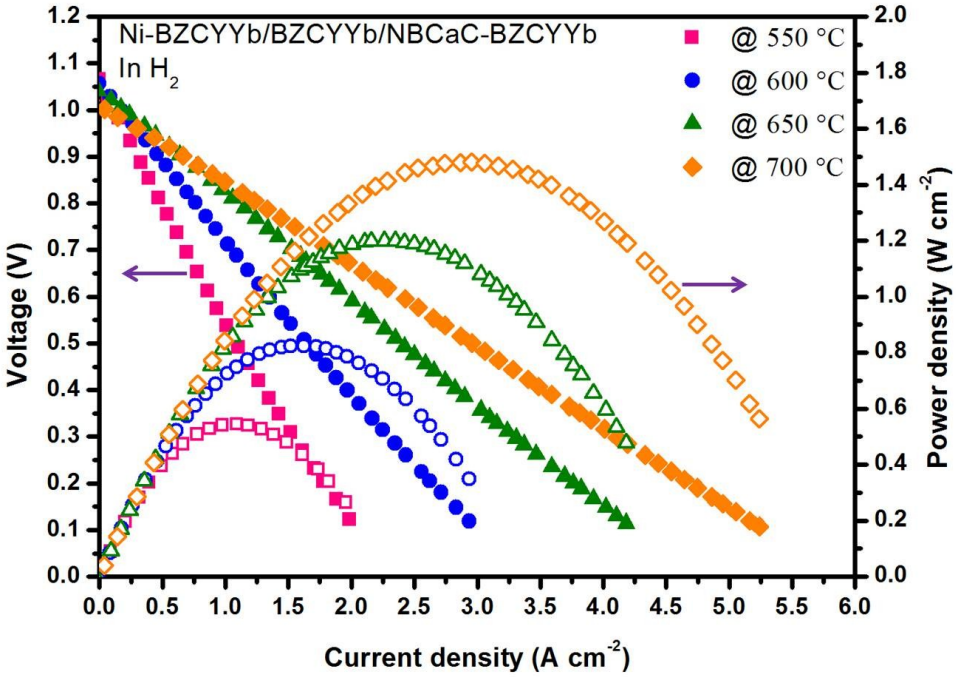

Figure S2. I-V and I-P curves of the conventional H-SOFC in H_2 at temperatures between 550 °C and 700 °C.

To assess the electrochemical performances of H-SOFC with conventional configuration, the cell configured as Ni-BZCYYb/BZCYYb/NBCaC-BZCYYb was first tested in pure hydrogen. In the corresponding I-V and power density plots shown in Fig. S2, the maximum power densities of the cell reached 544, 825, 1,199 and 1,480 mW cm^{-2} at 550, 600, 650 and 700 °C, respectively. The cell fabricated is indeed the state-of-the-art, showing the performances that are among the best reported in the literature to our best knowledge.

Figure S3

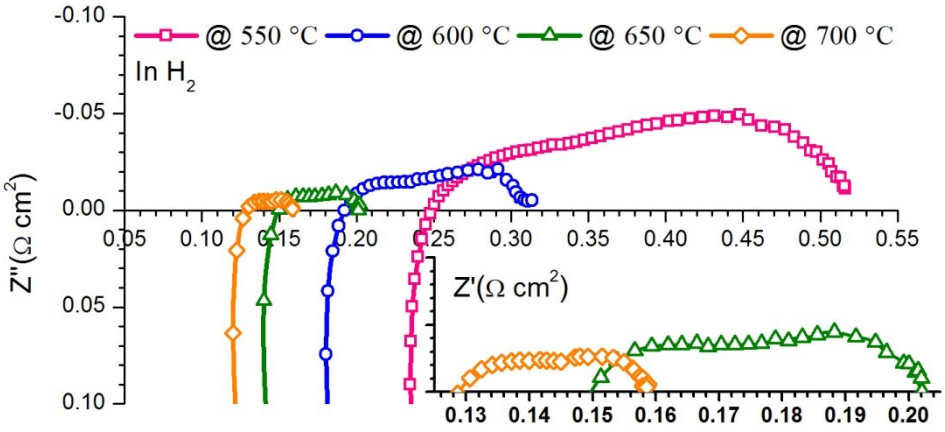

Figure S3. Electrochemical impedance spectra of the conventional H-SOFC in H_2 at temperatures between 550 °C and 700 °C.

As shown in the impedance spectra, the polarization resistances (R_P) of the cell were 0.266, 0.124, 0.052 and 0.031 Ω cm^2 at 550, 600, 650 and 700 °C, respectively.

Figure S4

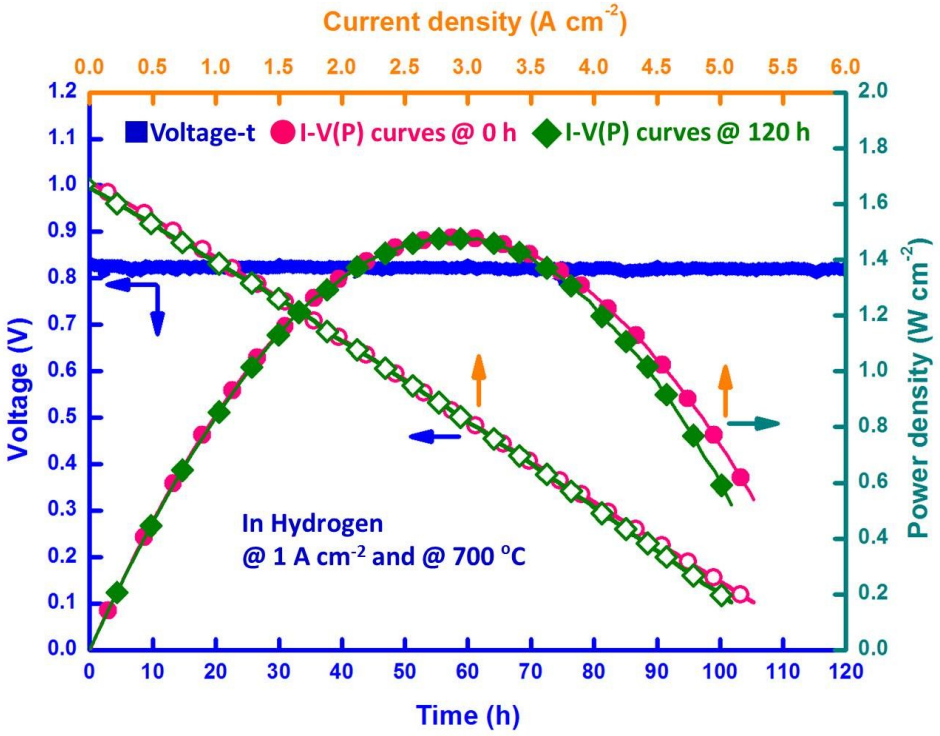

Figure S4. Voltage as a function of time for the cell, operated at 700 °C and at a constant current of 1 A cm^{-2} in H_2, and I-V and I-P curves of the same cell before and after the stability test.

Sequentially, we determined the long-term stability of the cell as shown in Fig. S4. The voltage of cell was recorded as a function of time under a constant current load of 1 A cm^{-2} at 700 °C. For comparison, the I-V and power density curves of the same cell before and after the 120 h stability test are also shown. After the stability test, negligible degradation was recorded, suggesting excellent electrochemical stability of the cell.

Figure S5

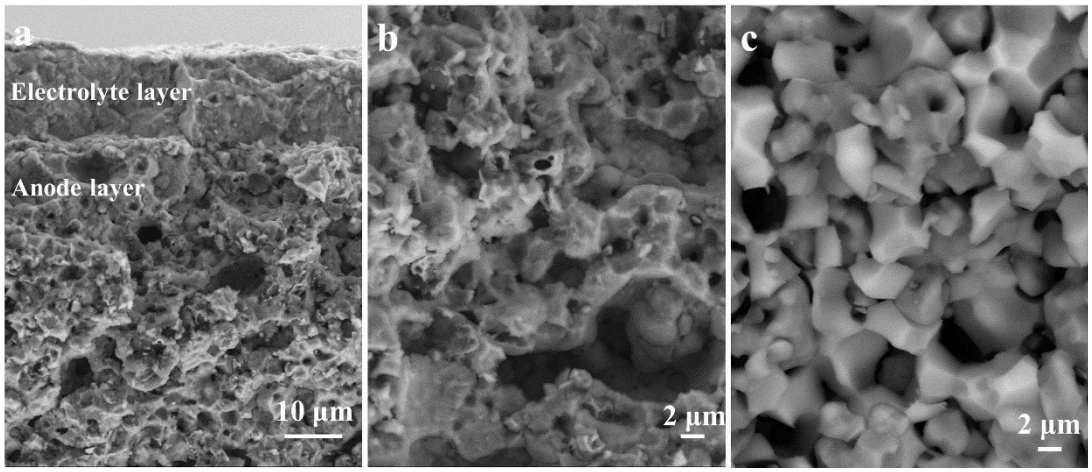

Figure S5. (a) The cross-sectional microstructure of the conventional H-SOFC after test in CH_4-CO_2; (b) the magnified image of the Ni-BZCYYb anode part of (a); (c) the microstructure of the as-reduced Ni-BZCYYb in H_2.

No carbon fibers were observed in the Ni-BZCYYb anode after test in CH_4-CO_2 (**a** and **b**). Compared to the as-reduced Ni-BZCYYb anode in H_2 (**c**), the surface of the Ni-BZCYYb anode and the BZCYYb electrolyte became significantly rougher after exposure to CH_4-CO_2, implying the formation of new phases.

Figure S6

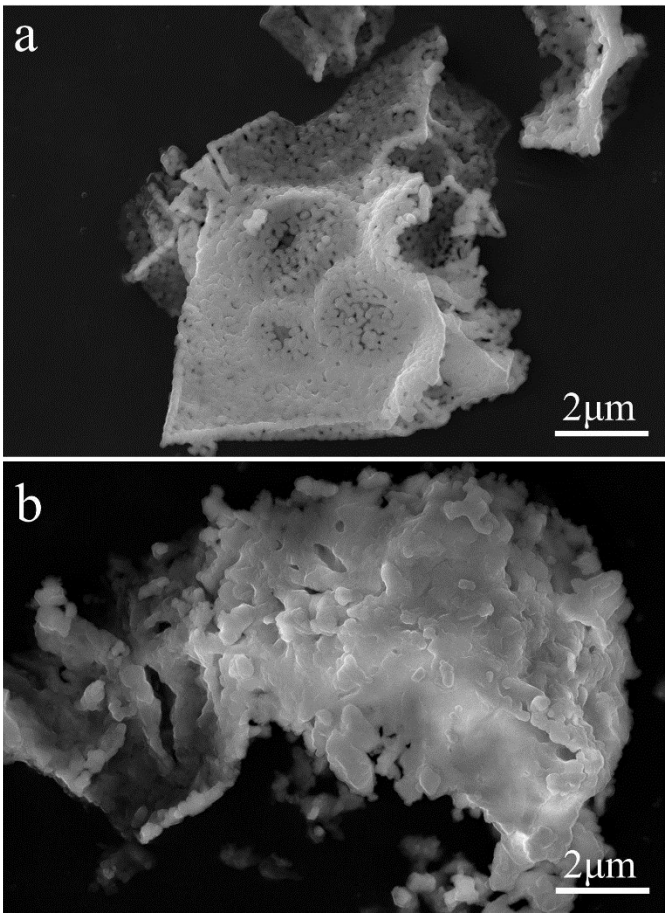

Figure S6. SEM images of BZCYYb powder after 24 h exposure at 700 °C in (a) air and (b) CH_4-CO_2.

Due to the decomposition of BZCYYb and formation of barium carbonate, the grain morphologies of the crystals in **b** changed. The bigger granular particles were likely the formed barium carbonate (*cf.* the XRD results). This result proved that the BZCYYb electrolyte is not stable in CH_4-CO_2.

Figure S7

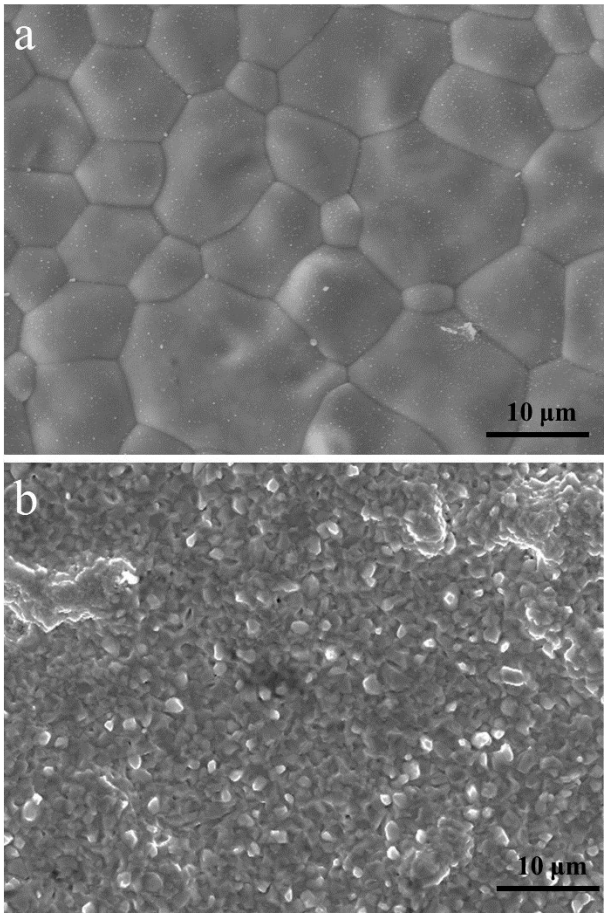

Figure S7. SEM images showing the surface microstructure of the sintered BZCYYb disk (a) before and (b) after being exposed to pure CO_2 at 700°C for 24 h.

In accordance with the previous results, the clear grain boundaries of the BZCYYb disappeared after being exposed to CO_2 and its surface became rougher, meaning that the BZCYYb was decomposed in CO_2 atmosphere.

Figure S8

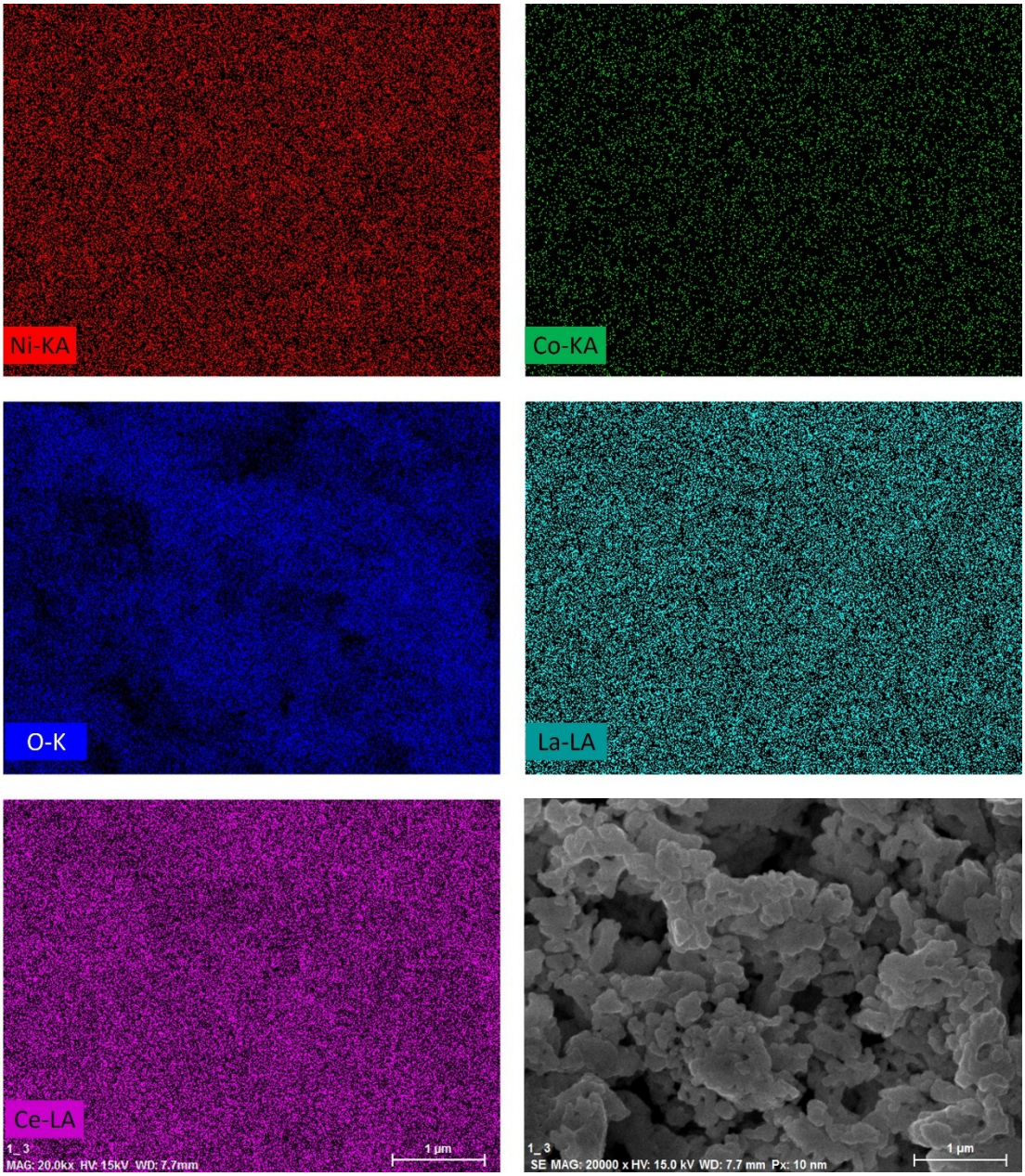

Figure S8. SEM and EDX mappings of the NiCo-LDC catalyst prepared by the GNP method.

It can be seen from the EDX mappings that uniform element distribution was obtained in the catalyst prepared by the GNP method.

Figure S9

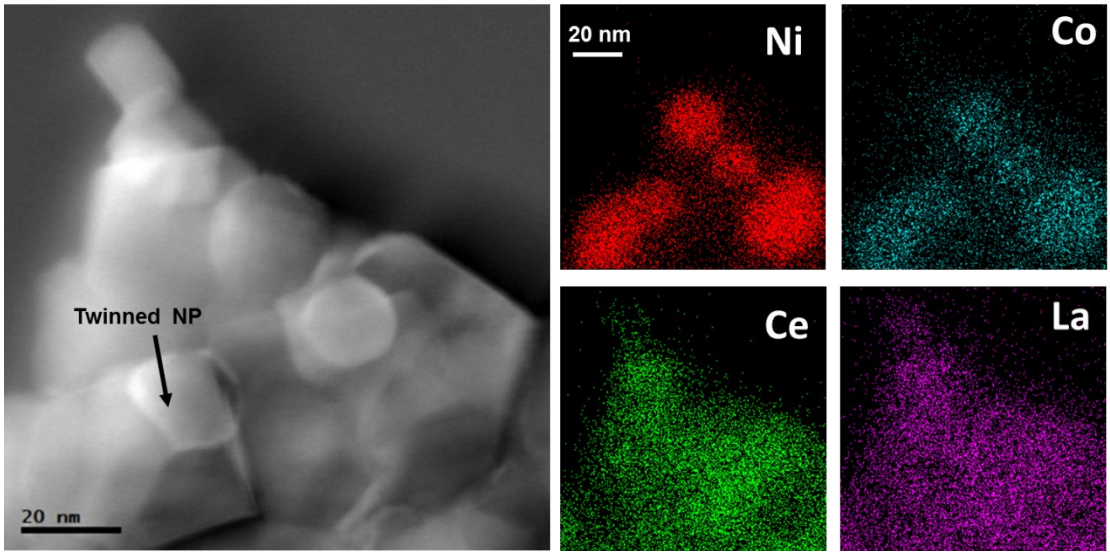

Figure S9. STEM-HAADF (high-angle annular dark field) image of NiCo-LDC sample prepared by GNP method showing twinned nanoparticles; and EDX elemental mappings of Ni, Co, Ce and La.

Ni and Co formed bimetallic nanoparticles (NP) with the particle size ranging from 15 to 30 nm, which were well-dispersed over cube-like LDC crystals.

Figure S10

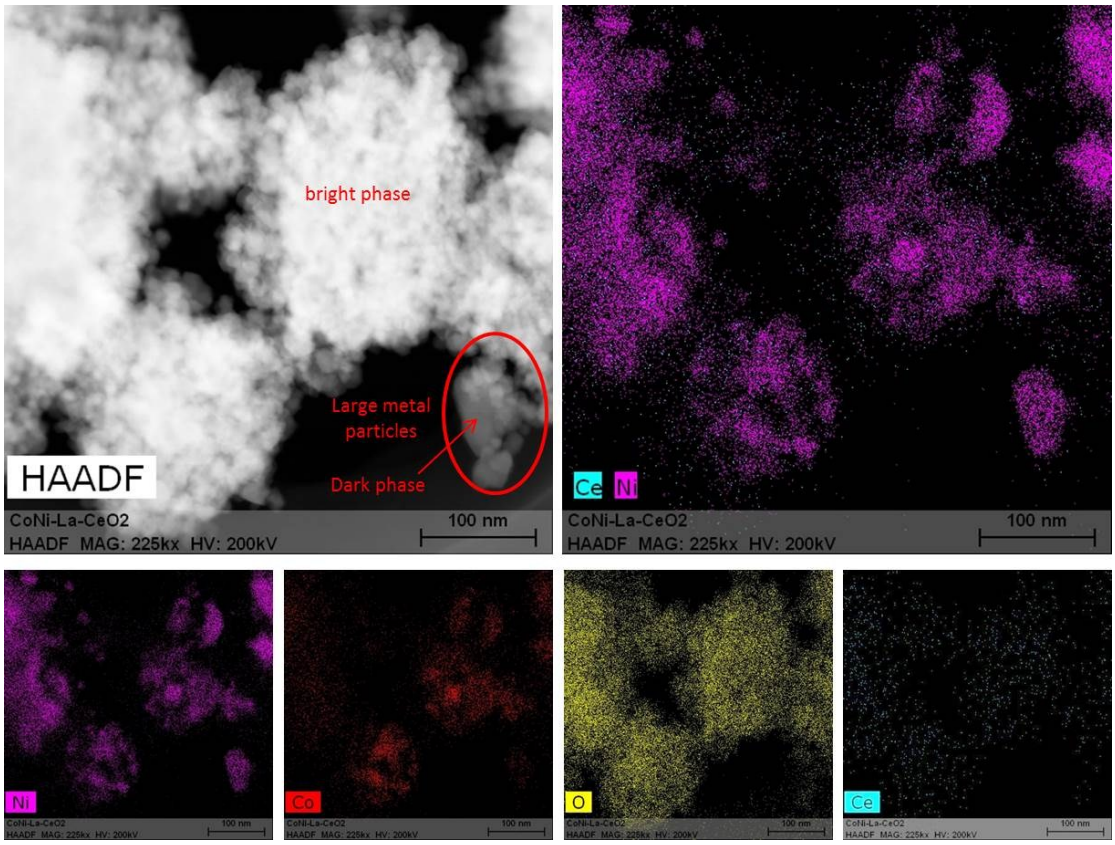

Figure S10. STEM-HAADF image of a NiCo-LDC sample prepared by the wet impregnation method; and EDX elemental mappings of Ni, Co, Ce and O.

In STEM-HAADF image, the dark phase is the NiCo metal and the bright phase is the LDC particles, due to the larger atomic number of Ce and La elements. After reduction in H_2, the NiCo nano particles agglomerated on LDC particles, forming large metal particle clusters sized from 50 nm to 200 nm.

Figure S11

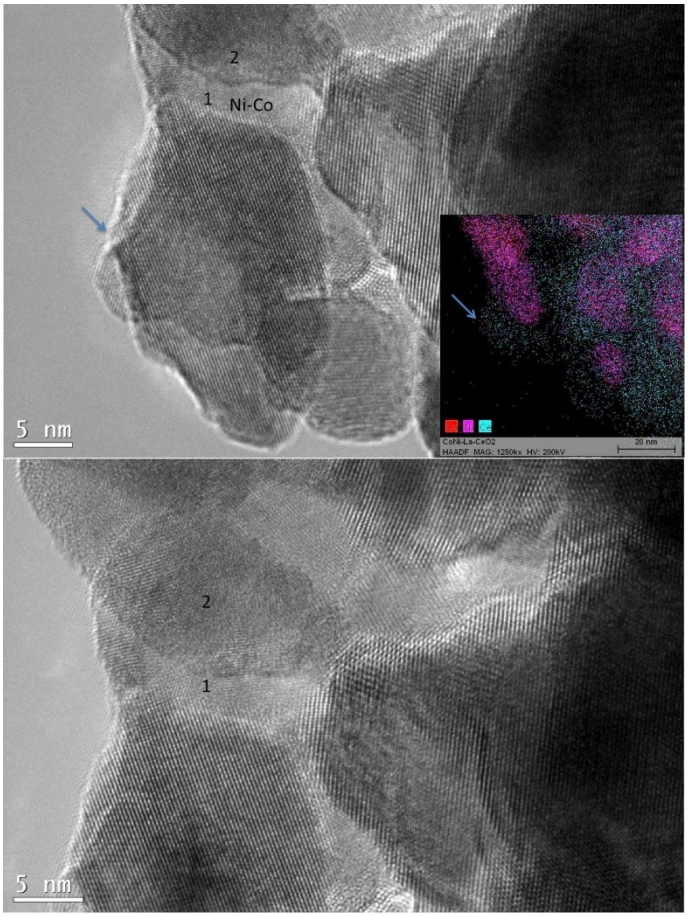

Figure S11. HRTEM images of catalyst prepared by the wet impregnation method and EDX elemental mapping of Ni, Co, Ce.

The NiCo particles severely agglomerated in the NiCo-LDC catalyst prepared via the wet impregnation method. The HRTEM image showed the closely situated NiCo nanoparticles forming a big cluster on LDC. Furthermore, these bimetallic had a semi-spherical morphology with few twinned structures.

Figure S12

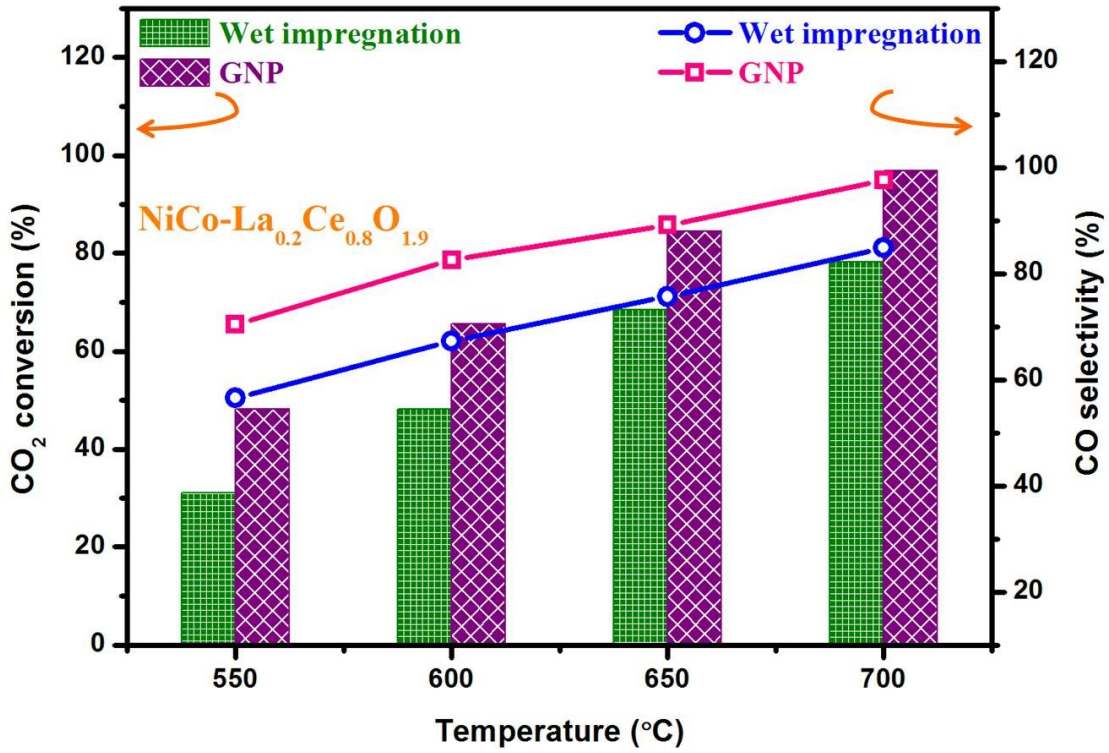

Figure S12. CO_2 conversion and CO selectivity comparisons of NiCo-LDC catalyst prepared by the two different methods in methane dry reforming reaction.

The catalyst prepared by GNP method possessed optimized microstructures and outperformed that derived from wet impregnation method.

Figure S13

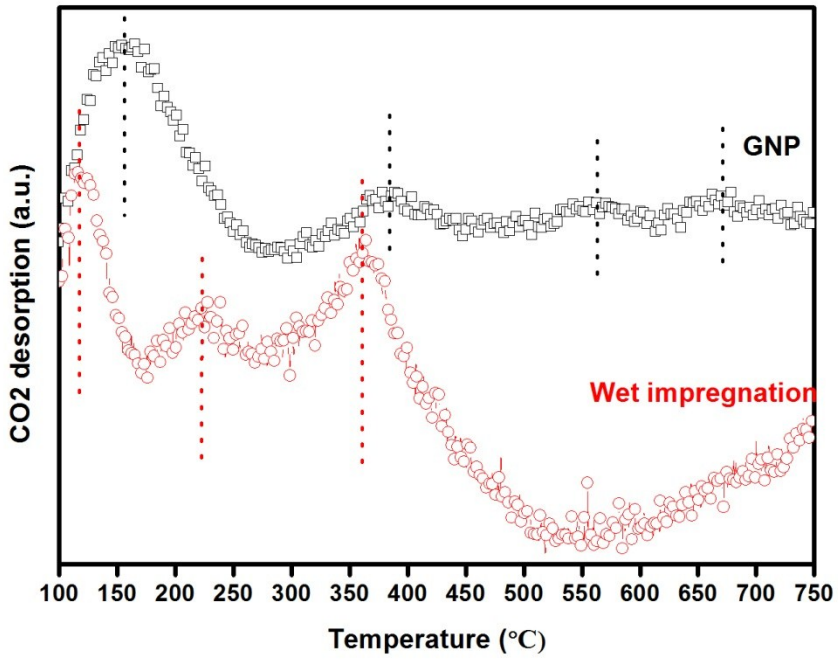

Figure S13. CO_2-TPD spectra of the two NiCo-LDC catalysts.

Usually, CO_2 can weakly bond with the catalyst, and the addition of La dopant enhanced the adsorption capability of the catalyst. Possibly due to the finer microstructure, NiCo-LDC prepared via GNP method showed higher volume of CO_2 adsorption.

Figure S14

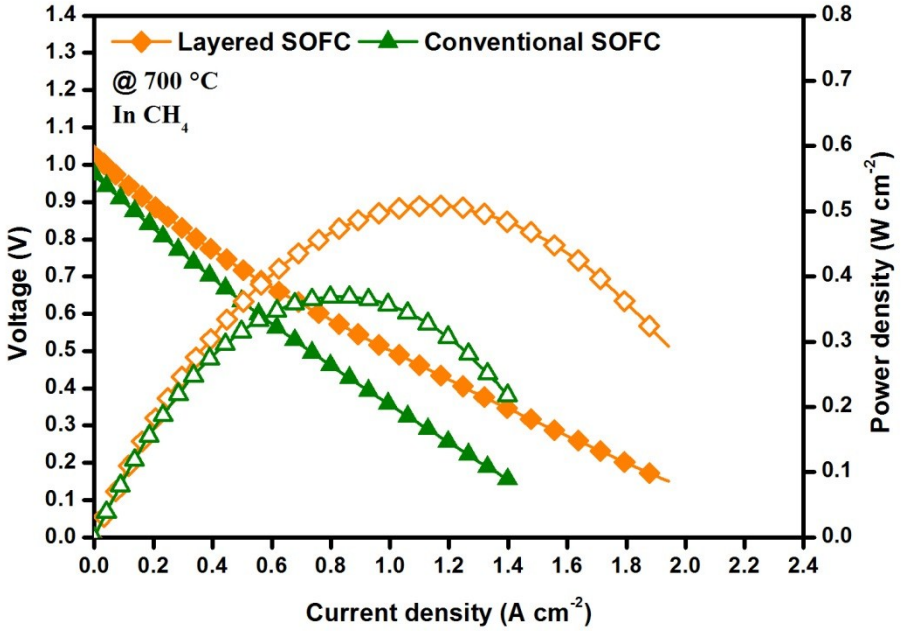

Figure S14. I-V and I-P curves of the conventional H-SOFC and layered SOFC in CH_4 at 700 °C.

When pure CH_4 was used as fuel, both the conventional and the layered H-SOFC demonstrated substantially decreased electrochemical performances, albeit they were comparable to some good O-SOFCs fueled with CH_4 [1-2]. Still, the layered H-SOFC also showed much better performances (higher OCV and power density) pertaining to the superior methane activation competence (presumably producing more H_2 via methane cracking).

Figure S15

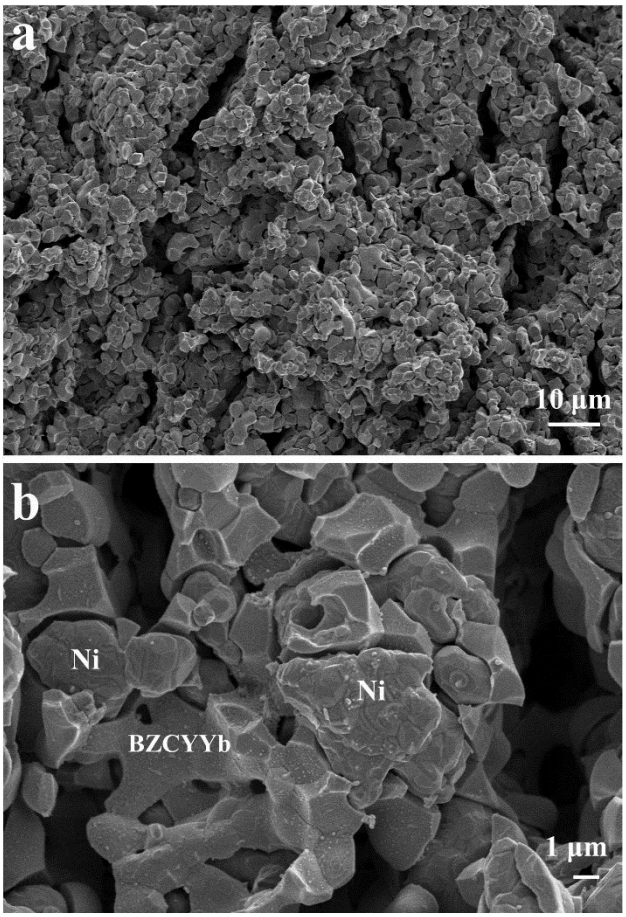

Figure S15. Microstructure of the Ni-BZCYYb anode of the layered SOFC after test in CH_4-CO_2 for 100 h.

No carbon deposition was visible from the SEM analysis. Furthermore, the microstructure of the Ni-BZCYYb was essentially identical to the fresh one (Fig. S5c). The "crack-like" structures in Fig. S15 are pores that were intentionally generated by adding pore formers.

Figure S16

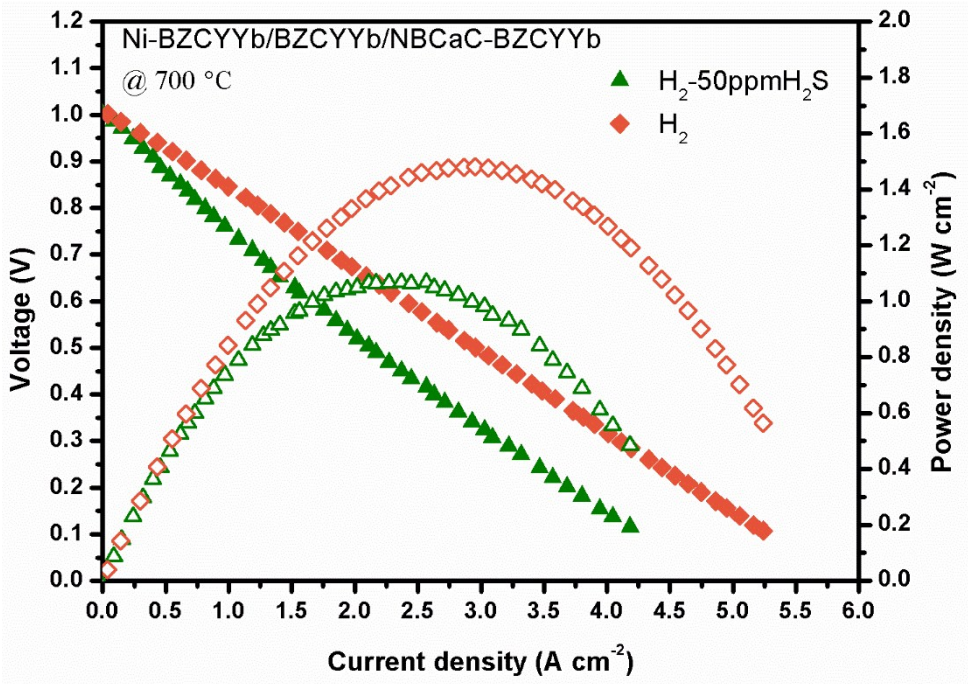

Figure S16. I-V and I-P curves of the conventional cell in H_2 and H_2-50ppm H_2S at 700 °C.

Figure S17

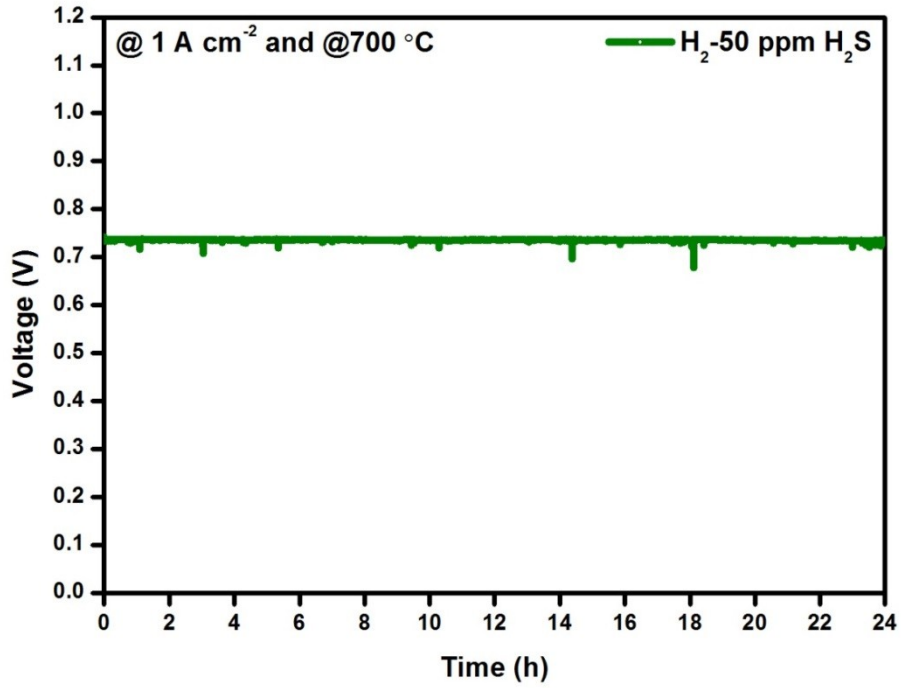

Figure S17. Voltage as a function of time for the conventional cell, operated at 700 °C and at a constant current of 1 A cm^{-2} in H_2-50ppm H_2S.

Reference

1. Z. Wang, Y. Li, J. Schwank, *Journal of Power Sources*, 2014, 248, 239-245.

2. Y. Chena, Y. Zhang, Y. Lin, Z. Yang, D. Su, M. Han, F. Chen, *Nano Energy*, 2014, 10, 1-9.